Materials Chemistry and Physics 132 (2012) 815–822

Contents lists available at SciVerse ScienceDirect

Materials Chemistry and Physics

journal homepage: www.elsevier.com/locate/matchemphys

Nanostructured Al/Al_4C_3 composites reinforced with graphite or fullerene and manufactured by mechanical milling and spark plasma sintering

F.C. Robles Hernández [a,*], H.A. Calderon [b]

[a] The University of Houston, Mechanical Engineering Technology, Houston, TX 77204, USA
[b] Departamento Ciencia de Materiales, ESFM-IPN, UPALM, Zacatenco, Mexico, DF 07338, Mexico

ARTICLE INFO

Article history:
Received 2 August 2010
Received in revised form 8 November 2011
Accepted 9 December 2011

Keywords:
Fullerene
Composites
Mechanical alloying
Phase transformation
Transmission Electron microscopy

ABSTRACT

Nanostructured Al matrix composites with reinforcements of graphite or fullerene (C_{60} + C_{70} + soot) have been produced by mechanical milling and spark plasma sintering (SPS). X-ray diffraction and transmission electron microscopy show that C_{60} + C_{70} withstand longer mechanical milling/alloying times than graphite. Fullerene is a good control agent during mechanical alloying resulting in a denser Al/fullerene composite when compared to the Al/graphite one. A refinement mechanism that takes place during mechanical alloying of fullerene and graphite is experimentally found and correspondingly discussed. Such a mechanism plays a major role in the amorphization of graphite. The larger surface area of the fullerene mix after milling promotes a better interaction with Al and hence allows its complete transformation into Al_4C_3 during the SPS process. The sintered products show an increase in hardness for the Al/fullerene composite of 6 times and only 4 times for the Al/graphite composite. The SPS technique shows to be an excellent method to transform the fullerene into Al_4C_3 while preserving its nanostructured nature.

Published by Elsevier B.V.

1. Introduction

The successful synthesis of fullerene and CNT has been reported by using different methods. It gives rise to interesting structures from buckyballs, buckytubes, onions, giant fullerene structures, concentric structures, etc. [1–5]. The most common structures (buckyballs) are C_{60} and C_{70}, they are composed of atomic arrangements of carbon into pentagons and hexagons [2]. More recently Terrones and Terrones proposed a structure that includes also heptagons [6]. Conventionally, the fullerenes are synthesized by using high intensity lasers or electric arcs and commonly enriched by the method proposed by Krätschmer et al. [7]. The reported mechanical properties of C_{60}, C_{70} and CNTs are outstanding and can reach Young moduli between 400 GPa and 4150 GPa [1,8] and compressive strengths between 100 and 150 GPa [1,9]. Some uses of fullerenes are: reinforcement and as nanostruders [10–13].

The dispersion of carbides (e.g. Al_4C_3) in Al matrices has been successful by different methods including, but not limited to: reaction milling, thixocasting, rheocasting, electromagnetic stirring and metal infiltration [10,14–19]. On the other hand, the production of nanostructured Al matrix composites reinforced with carbon nanoparticles (e.g. fullerene, MWCNT, etc.) is controversial [1,10,21–26]. The following are the two effects reported when carbon nanoparticles are used as reinforcement for Al matrix composites: (*i*) the formation of carbides and (*ii*) when CNTs are added in small amounts (<2%) they act as effective reinforcements with limited to no chemical interaction. In either case increases in mechanical, and electrical properties are observed. Some improvements in mechanical properties are usually observed when the Al_4C_3 is formed; however, better electrical conductivity is observed in the absence of chemical bonding among Al and carbon. Some of the challenges to produce nanostructured Al matrix composites reinforced with carbon nanoparticles include the segregation of the CNTs and their cost. The above has motivated the present research work in the use of carbon soot (fullerene mix) instead of pristine carbon nanoparticles. In fact, carbon soot has a similar graphene-like structure as the observed in carbon nanostructures and is considerably cheaper.

Mechanical alloying is a method originally proposed by Gilman and Benjamin [17–19] in the 60s. This method has proven to be successful to manufacture nanostructured materials at room temperature [10–19]. One of the advantages of mechanical alloying is that varying time and temperature is possible to promote or hinder phase transformation of components including ductile metals such as aluminum [20]. Mechanical alloying is an excellent method to produce nanostructured and highly homogeneous powders of a large number of sizes and of different compositions. In order to preserve the nanostructured nature of the mechanically alloyed powders, low temperatures, short times and high pressures are

* Corresponding author. Tel.: +1 713 743 6147; fax: +1 505 213 7106.
E-mail address: fcrobles@uh.edu (F.C. Robles Hernández).

0254-0584/$ – see front matter. Published by Elsevier B.V.
doi:10.1016/j.matchemphys.2011.12.017

ideal for sintering. These conditions are combined in the Spark Plasma Sintering (SPS) that makes it a promising method to produce highly/fully dense nanocrystalline composites [12].

In the present work mechanical alloying and SPS are combined to produce nanostructured composites of Al/graphite and Al/fullerene. The characterization is conducted by means of Scanning Electron Microscopy (SEM), X-Ray Diffraction (XRD) and Transmission Electron Microscopy (TEM), hardness measurements have been also performed as per indicated in the respective ASTM standard.

2. Experimental procedure and materials

Powders of Al (99.9 at.% purity and a particle size < 180 μm), graphite (99.9 at.% purity and a particle size < 5 μm) and fullerene mix (21 at.% C_{60} + 9 at.% C_{70} + 70 at.% soot), are used as starting materials. The mixture of fullerene mix contains a minimum of 30 at.% $C_{C60+C70}$. In the present paper the C_{60} + C_{70} + soot mixture (commercially known as "Carbon Soot") is referred as fullerene and has been obtained from STEM Chemicals. The rest of the non-C_{60} + C_{70} carbon present in the fullerene mix is called soot. Nanostructured Al based composites have been prepared with two different components i.e., Al/graphite and Al/fullerene. In both cases, 15.7 at.%C is added to the Al base powders. The term original sample is used to refer to the mixed powders before mechanical alloying. The idea of using the fullerene mix is to demonstrate its effectiveness and SPS to form a nanostructured Al/Al_4C_3 composite.

Mechanical milling (for pure graphite and fullerene) has been conducted in a Spex mill while mechanical alloying (for Al/graphite or Al/fullerene composites) is carried out using a horizontal ball mill. Mechanical milling has been conducted for up to 3.5 h and mechanical alloying for 100 h. Based on previous experience comparable microstructures can be obtained by using the above times in Spex and ball milling [11,12]. Mechanical alloying at intermediate times between 0 and 100 h has also been conducted, but due to the significance to this paper only the results of 100 h of mechanical alloying are presented and discussed. The ball to powder weight ratio during milling was 8:1 and 100:1 for Spex and ball milling respectively. Ethanol is added in the Spex mill as a control agent and no control agent is added in the ball mill. The manipulation of the powders has been kept in a controlled atmosphere (Ar) environment to prevent any degradation of the powders or potential reactions before or during the milling process with oxygen or nitrogen.

The alloyed powders have been SPS sintered at 773 K, 100 MPa for 600 s at a heating rate of 3.3 K/s. The dimensions of the sintered samples are 13 mm in diameter and 5 mm in thickness. The sintered products are polished by following standard procedures for microhardness testing. The micro-hardness test has been conducted on a Leco-LM700 apparatus with an applied load of 10 N for 10 s. The reported values are the average of 20 measurements made in the aluminum matrix.

X-ray diffraction (XRD) has been conducted in a SIEMENS D5000 diffractometer equipped with a Cu tube with a characteristic K_α, λ = 0.15406 nm. The grain size is determined using the Scherrer method and the reflections (1 1 1), (1 1 1), (0 0 2) and (8 0 0) for Al, C_{60}/C_{70}, graphite and Al_4C_3 respectively. The Scherrer method was selected due to its higher accuracy (±15%) over other methods; such as, the Integral breath, Warren-Averbach methods when they are compared to Transmission Electron Microscopy (TEM) (TEM) [27]. The same reflections are used to determine the lattice parameters. The SEM observations have been carried out on a JSFM35CF JEOL apparatus equipped with an Energy Dispersive X-ray Spectroscopy (EDS) operated at 20 kV and TEM is conducted on a JEOL JEM200FXII. For TEM, the samples are prepared by dispersing the powders in ethanol to form a dilute suspension from which an aliquot is taken and deposited on a Cu-graphite 300 mesh grid. The as sintered products are surface polished for SEM, and electropolished on a double jet electropolisher for TEM, the electropolishing is conducted at 230 K using an electrolyte of 25 vol% HNO_3 and 75 vol% CH_3OH. The magnification and electron diffraction patterns were calibrated in the TEM using a gold replica and standard procedures were followed.

3. Results

Table 1 shows the values of the respective grain size, and lattice parameters for all systems in as mixed or milled conditions. Table 1 summarizes the changes in lattice parameters resulting from the effects of mechanical milling/alloying for each constituent of the composites. The changes in lattice parameters were determined

Table 1
Crystalline characteristics of materials as determined by XRD results of graphite, fullerene, and for the original, mechanically milled, mechanically alloyed and sintered samples. All units in nm.

Commercial fullerene (nm)						
C_{60}	1.437					
C_{70}	1.924					
Mechanical milling						
	0 h		1 h		2 h	3.5 h
Graphite (XRD)						
Lattice parameter						
a	0.213		0.214		0.214	0.214
c	0.674		0.671		0.672	0.670
Particle diameter	3.675		2.845		0.836	0.530
Mechanical milling						
	0 h for C_{60}		0 h for C_{70}		0 h for C_{60+70}	
Fullerene (XRD)						
Lattice parameter	1.424		1.921		1.458	
Grain Size	1.568		1.407		1.185	
Fullerene (TEM)						
Lattice parameter	1.428		N/A		1.185	
Mechanical alloying						
			0 h			100 h
Al-$C_{graphite}$ system						
Lattice parameter (Al)			0.408			0.405
Grain size (Al)			18.34			13.51
Mechanical alloying						
	0 h		100 h			
	a_{XRD}	c_{XRD}	a_{XRD}	a_{TEM}	c_{XRD}	c_{TEM}
Lattice Parameter (graphite)	0.201	0.678	0.207	0.2363	0.714	0.669
Grain size	1.162				0.693	
Mechanical alloying						
			0 h			100 h
Al-C_sub fullerene system						
Lattice parameter (Al)			0.408			0.405
Grain size (Al)			18.94			13.52
Mechanical alloying						
	0 h			100 h		
	a_{XRD}	a_{TEM}		a_{XRD}	a_{TEM}	
Lattice Parameter (fullerene)	1.420	1.428			1.459 ± 0.25	
Grain size	15.77			14.12		

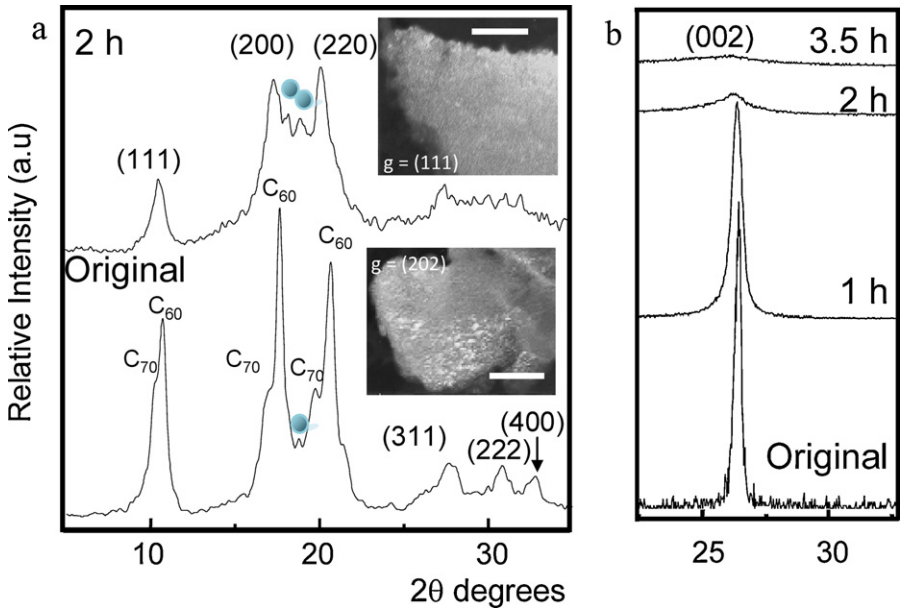

Fig. 1. XRD patterns of (a) fullerene and (b) graphite milled using a Spex for different times. Inserts showing the respective TEM dark field images. Scale bar 100 nm. Unidentified phase by means of XRD.

per XRD and TEM analysis. Milled graphite has not been analyzed by TEM.

Fig. 1 shows the XRD patterns for fullerene, and graphite before and after Spex milling for 2 and 3.5 h respectively. The XRD spectrum of the original fullerene mix shows the presence of C_{60} and C_{70}; having C_{60} as the most intense reflection owing to the ratio of C_{60} and C_{70} in the original powders. The reflections indicated with a circle have been previously identified as fullerene with a tetragonal crystalline structure [21]. In Ref. [22,40] is shown by TEM that one of the alternatives is likely to be the presence of tetragonal C_{60} in the mechanically alloyed Fe-fullerene system. After mechanical milling only the presence of a family of fullerene reflections is prevalent and corresponds to C_{60} with small reflections that match with the rombohedral and tetragonal fullerene structures. This indicates that both, C_{60} and C_{70}, are mixed forming a combined crystalline structure.

Previous investigations have reported that mechanical milling of C_{60} promotes the transformation to C_{120} and if a long enough milling time is allowed polymeric transformations can occur [24]. However, in this work the milling time is not sufficient to promote such a transformation(s). The nanostructure nature of the raw and milled fullerene can be observed in the insets shown in Fig. 1a. The amorphization of graphite becomes apparent from the XRD while the fullerene withstands the 2 h of mechanical treatment without apparent changes. The XRD results of graphite (Fig. 1b) show the (0 0 2) reflection with a noticeable reduction in intensity as the milling time increases and at 3.5 h of milling this reflection is almost extinct suggesting that for this milling time graphite is quasi-amorphous.

The SEM images in Fig. 2 illustrate mechanically alloyed powders for the Al/graphite and Al/fullerene composites after 100 h of mechanical alloying showing their relative agglomeration and particle size. The powders of the Al/fullerene composite have clearly smaller sizes with a more normal size distribution and irregular shapes than the Al/graphite composite. Additionally, agglomeration is more pronounced for the Al/graphite composite. The "control agent" effect observed in graphite has been previously reported [11]. Such effect prevents the welding among particles and with the milling media. By comparing the particles in Fig. 2a and b, it can be said that the fullerene mix is more effective as a control agent than graphite. This can be attributed to its crystalline structure (*fcc*) with more slip systems than graphite, but most importantly the presence of the soot that is produced parallel to the (1 1 1) plane. The glide of atomic planes or dislocations along the graphenes-like structures present in the fullerene mix has a lubricity effect that act as a control agent.

In Fig. 3a and b, XRD diffractograms are given for the Al/fullerene and Al/graphite composites before and after mechanical alloying. The diffractograms in Fig. 3a present two spectrums for the original sample; in the first one the intensity is in decimal scale and, in the second one, it is in a logarithmic scale. The logarithmic scale is used to better visualize the peaks corresponding to graphite

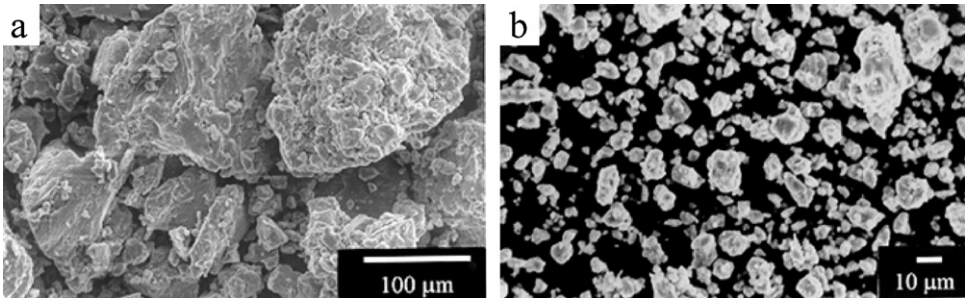

Fig. 2. SEM images of the (a) Al/graphite and (b) Al/fullerene mechanically alloyed powders for 100 h in ball mill.

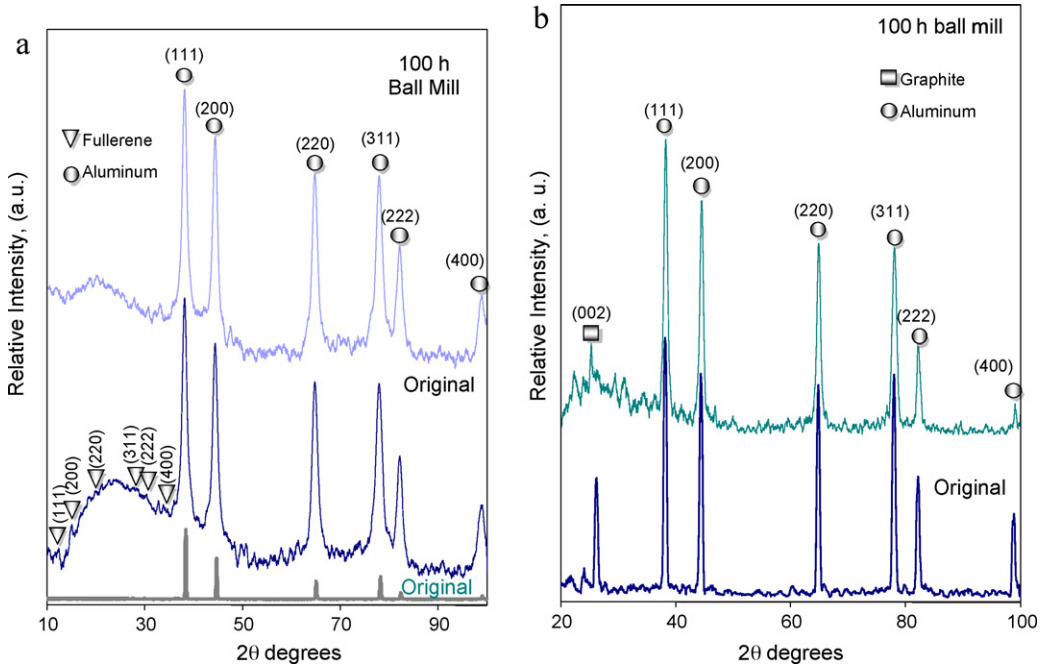

Fig. 3. XRD patterns of the original powder mixture and the as-milled (100 h) samples for (a) Al/fullerene and (b) Al/graphite systems. Note; two diffractograms for the original sample are presented to compare the advantage of using a logarithmic scale (lower) instead of a decimal scale (upper).

and fullerene present in the respective composites, which in turn simplifies its identification without affecting the 2θ scale. The 2θ positions of the peaks are used to determine the lattice parameter and the peak shape for the grain size. In Fig. 3b it can be seen that after 100 h of mechanical alloying, the intensity of the graphite peaks become rather weak. The grain size results given Table 1 show that the Spex milled graphite for 3.5 h and the graphite in the mechanically alloyed composite for 100 h are similar. On the other hand the grain size for the Al/fullerene composite milled fullerene after 100 h is comparable to that of the Spex milled fullerene for 2 h. On such a basis, apparently Al is assisting the grain refinement of graphite, but has a negligible effect on fullerene.

The low intensity of the peaks for graphite or fullerene observed in Fig. 3 can be attributed to several factors such as the volume ratio Al:graphite or Al:fullerene in the composites and the effect of milling on the structure of both carbon phases. The volume fraction of carbon phases in the present research can be considered low. Additionally, experimental evidence shows that fullerene is more resistant to mechanical alloying or milling than graphite. After 100 h of milling the presence of fullerene is still clear as seen in the XRD results. The crystal quality of the Spex milled fullerene for 3.5 h is similar to that of the raw sample. Table 1 shows that the lattice parameter for Al is almost constant for all systems before and after mechanical alloying. Since the difference in atomic radii between Carbon and Al is very large and the formation of new phases starts at relatively low carbon contents, then any change in lattice parameter is attributed to plastic deformation (e.g. ratcheting).

Fig. 4 shows TEM dark field images and Selected Area Diffraction Patterns (SADP) corresponding to the as milled Al/graphite and

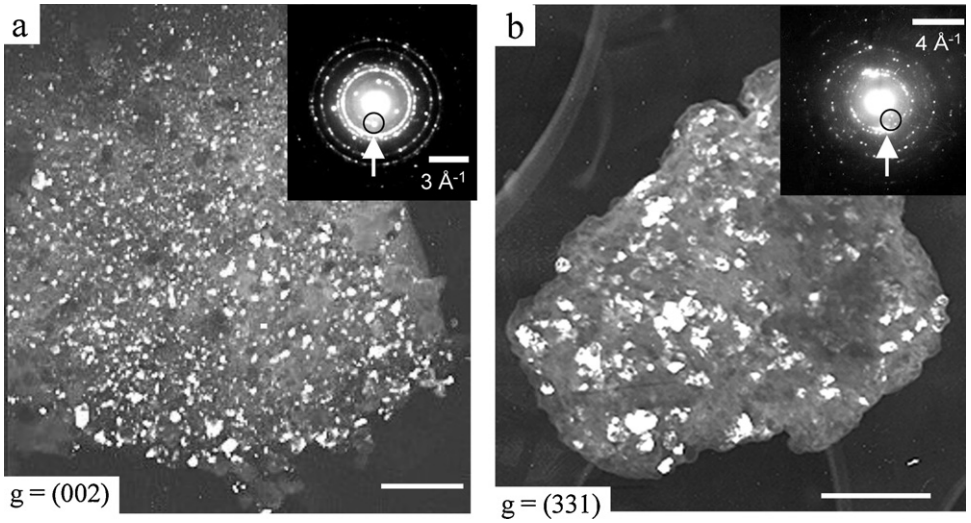

Fig. 4. TEM dark field micrographs and their respective SAD patterns after milling for 100 h for (a) Al/graphite and (b) Al/fullerene. Bright zones correspond to graphite or C_{60} respectively. Scale bar 200 nm. The arrow and circles are used to identify the reflection used for the dark field.

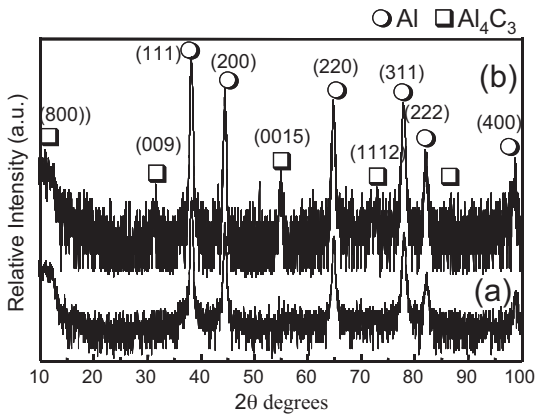

Fig. 5. XRD results of the as-sintered samples for the (a) Al/graphite, (b) Al/fullerene systems.

Al/fullerene composites. The use of the indicated reflections (*g*) produces the bright areas in the images corresponding to graphite or C_{60} respectively. From Fig. 4, it can be observed that the powders of either composite are highly homogeneous. The bright zones for the Al/graphite composite confirm the approximate grain size as determined by Scherrer and presented in Table 1 based on XRD results (Figs. 1 and 3). From the dark fields, it is observed that the amount of carbon (bright regions) particles in the Al/fullerene composite appears to be lower than in the Al/graphite composite. This is attributed to the lower volume fraction of C_{60} present in the fullerene mixture when compared to graphite. Table 1 gives the values of particle size and lattice parameters for the identified phases.

Fig. 5 presents the XRD results of SPS sintered samples. Fig. 5a shows that sintering sponsors the transformation of graphite into Al_4C_3. The XRD results for the Al/fullerene system show more reflections of Al_4C_3 and with higher intensity. This suggests that transformation of the carbon species is more efficient for the Al/fullerene system. The XRD results show no evidences of fullerenes peaks that is in agreement with the TEM findings.

Fig. 6 shows SEM and TEM images of the sintered products [29,40]. There are two major findings to observe in Fig. 6a-b, the larger and more abundant particles of Al_4C_3 (encircled for easy identification) in the Al/fullerene when compared to the Al/graphite composite. The composition of the Al_4C_3 particles has been verified by means of EDS. Both observations allow confirming the XRD results (Fig. 5) with a partial transformation of carbon phases in the Al/graphite composite and the complete transformation of carbon in the Al/fullerene system. These results are in agreement with previous reports [11,12,36].

Table 2 summarizes the Vickers microhardness results for the composites. Refs. [10,24] report values for Vickers microhardness of pure mechanically milled aluminum with values between 21 μHV (raw element [10]) and 50 μHV (mechanically milled and SPS sintered [24]). The results in Table 2 show increments of 375% and 582% for the Al/graphite and Al/fullerene composite with respect to the previously reported values [24]. The Al/fullerene system has a higher hardness that is attributed to the larger amount of Al_4C_3 formed during the sintering.

Table 2
Microhardness and calculated Rockwell B hardness results for the SPS samples.

Al-$C_{Graphite}$		Al-$C_{Fullerene}$	
μHV_{25}	HRB	μHV_{25}	HRB
188.24 ± 49	86.843 ± 19	291.97 ± 38	104.12 ± 14

The particles present in the Al/graphite composite (Fig. 6c, d) are composed by a mix of nanostructured crystals of Al_4C_3 and Al. The presence of graphite in the composite is not evident (Fig. 6d) due to its quasi amorphous nature that can be observed as diffuse ring(s). Fig. 7b shows an amorphous graphite particle identified in the Al/Graphite composite. The Al/fullerene composite shows that this composite is made of particles of either Al (Fig. 6e) or Al_4C_3 (Fig. 6f) and no evidence of free carbon in the form of C_{60} or C_{70} was found. The above results are in agreement with XRD results as presented in Fig. 5. The phases identified in the Al/graphite composite are: Al, Al_4C_3 and graphite. As for the Al/fullerene composite the phases are: Al and Al_4C_3. Fig. 6 demonstrates that both composites are nanostructured even after themomechanical processing (mechanical milling and SPS). This exhibits the potential of these methods to produce nanostructured composites.

The TEM bright field images given in Fig. 7a,b correspond to C_{60} and amorphous graphite found in the Al/fullerene (as-milled powder) and the Al/graphite (as-sintered) composites, respectively. These images are given as an evidence of the crystalline and amorphous nature of the reinforcements used in each system. The fullerene particle can still be found after milling, while the amorphous graphite is present in the composite in the as sintered sample. This demonstrates the higher resistance of C_{60} to amorphization when compared to graphite. The identified C_{60} particle is unique having a size of approximately 1 μm while the rest of the C_{60} observed in the composite is nanometric as shown in the respective dark field images and the XRD results (Table 1). There are two reasons for the presence of this relatively large C_{60} particle: (*i*) the typical size distribution in milled products [20] and (*ii*) the outstanding mechanical properties of carbon nanostructures (e.g. C_{60}, C_{70}, etc.).

The graphite particle in Fig. 7b is representative of the graphite present in the Al/graphite composite before and after mechanical alloying and SPS. This confirms the short range order of the graphite identified by XRD proving that the carbon present in this composite is amorphous. This raises the question about whether or not the graphite grains need to be large enough to hold a crystalline structure and being able to transform into Al_4C_3. If this is the case, there is a possibility that short-to-medium range order graphite particles cannot combine with Al to form Al_4C_3 explaining the reasons for the limited amount of this phase in the Al/graphite composite.

4. Discussion of results

In the following, an analysis is presented regarding the number of lattice cells in an average graphite grain before and after milling in a Spex mill. This is later compared to the characteristics of the mechanically ball milled graphite to understand the role of aluminum in the extra refinement of graphite when compared to fullerene in their respective composites. This analysis provides an explanation about the higher reactivity of fullerene during the SPS process. The determination of the number of lattice cells is calculated based on the results given in Table 1. The number of lattice cells present in an average grain of raw graphite is approximately $17 \times 17 \times 5$ along the "a_1,a_2" and "*c*" axis, respectively, i.e. an average particle size of 3.675 nm as given in Table 1. This corresponds to more than 1400 lattice unit cells per grain. After 2 h of Spex milling, the average size is reduced to approximately $8 \times 8 \times 3$ (i.e., 201 lattice unit cells) per grain. After 3.5 h of mechanical milling, graphite has short to medium range order along the "*c*" axis with a grain size of 0.53 nm; it means that these particles are smaller than their "*c*" cell dimension, thus a single crystal contains up to 30 atoms. In other words, after 3.5 h of Spex milling graphite is mainly a quasi-amorphous to amorphous matter that is demonstrated by electron diffraction (XRD and TEM) as well as the insets in Fig. 1a.

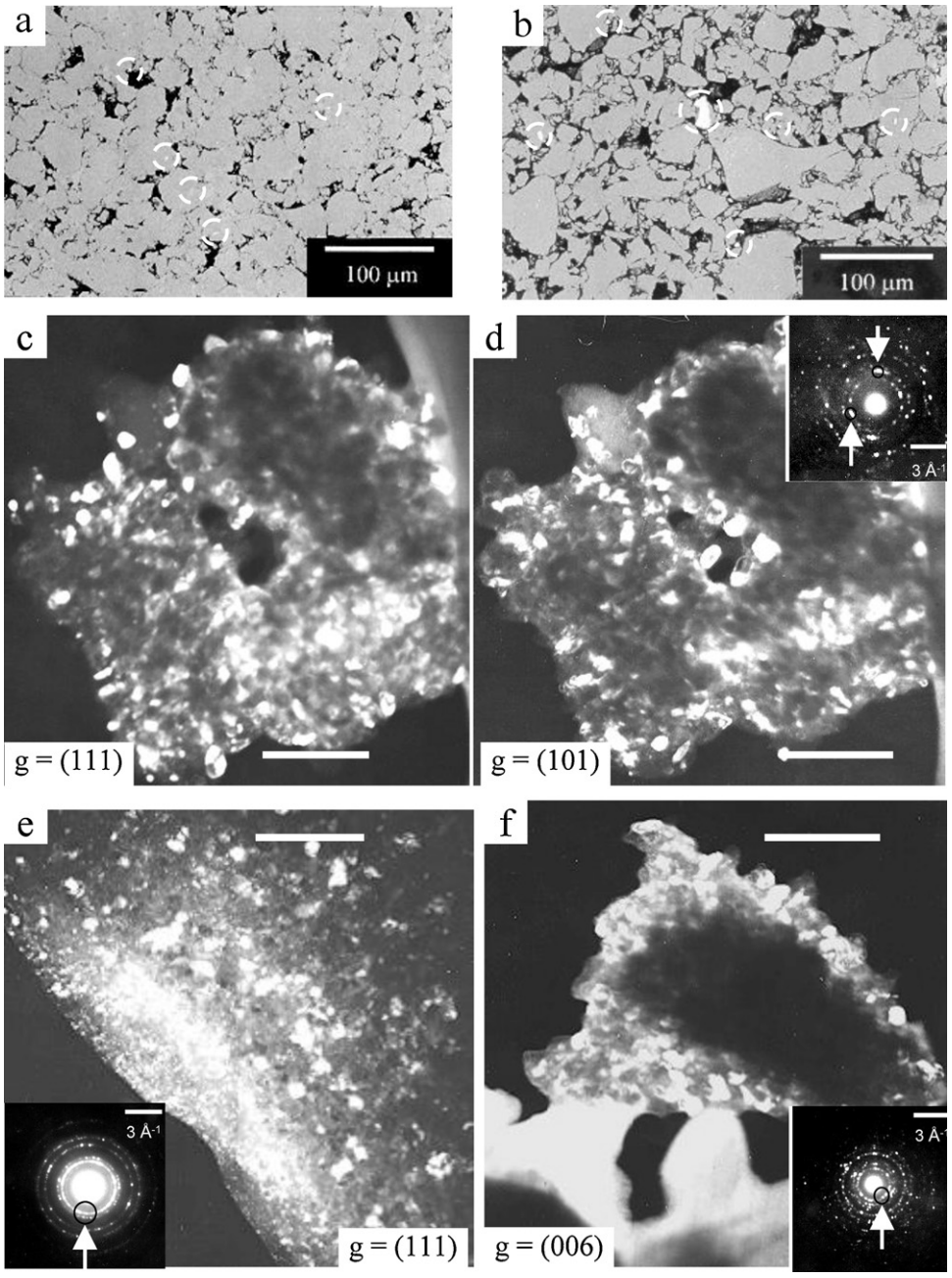

Fig. 6. (a,b) SEM images and (c-f) TEM dark field images corresponding to the sintered Al/graphite (a,c,d) and Al/fullerene (b,e,f) composites. The Al_4C_3 particles formed during the SPS process are indicated by circles in (a,b). TEM dark field images in (c,e) are obtained with Al Matrix reflections and (d,f) with Al_4C_3 reflections. Scale bar 200 nm.

Comparing the results in Table 1 one can understand that the graphite grain size after Spex milling for 3.5 h is similar to that after ball milling for 100 h. The grain size in the fullerene mix is found to be comparable for 2 h of Spex milling and 100 h of mechanical alloying. This is an indication that Al is somehow contributing in the further refinement of graphite, which can be attributed to the larger number of slip systems of the *fcc* (Al) cell when compared to the *hcp* (graphite) cell (i.e. 12 vs. and 2 slip systems per lattice). At the micro level stresses are transmitted in shear (dislocations glide and slip) and this is independent on how the stress is applied at the macro-level. Therefore, during the mechanical alloying the Al planes glide in the form of dislocations creating shear components that crash the graphite particles resulting in the extra refinement/amorphization of graphite.

The different surface area of the as milled graphite can explain the different activity of carbon in the composites. After mechanical alloying the graphite in the composite is composed of broken graphite-like structures with "*ab* or *ba*" stacking (low to medium range order, A9 structure, sp^2 bonding) instead of the typical "*aba*" stacking of an *hcp* system. Therefore, the carbon particles form aggregates with uneven surfaces prevent the contact/interaction with Al. In contrast, the soot is mainly composed by graphene-like layers allowing interaction from both sides with Al.

The C_{60} and C_{70} are highly reactive and due to its grain size and exposed surface area the reactions with Al are promoted during SPS ensuring the formation of the Al_4C_3 carbide. This and the relatively high homologous temperature during the SPS process ($T/\mathrm{Tm} \approx 0.8$) lead to the complete transformation of carbon into

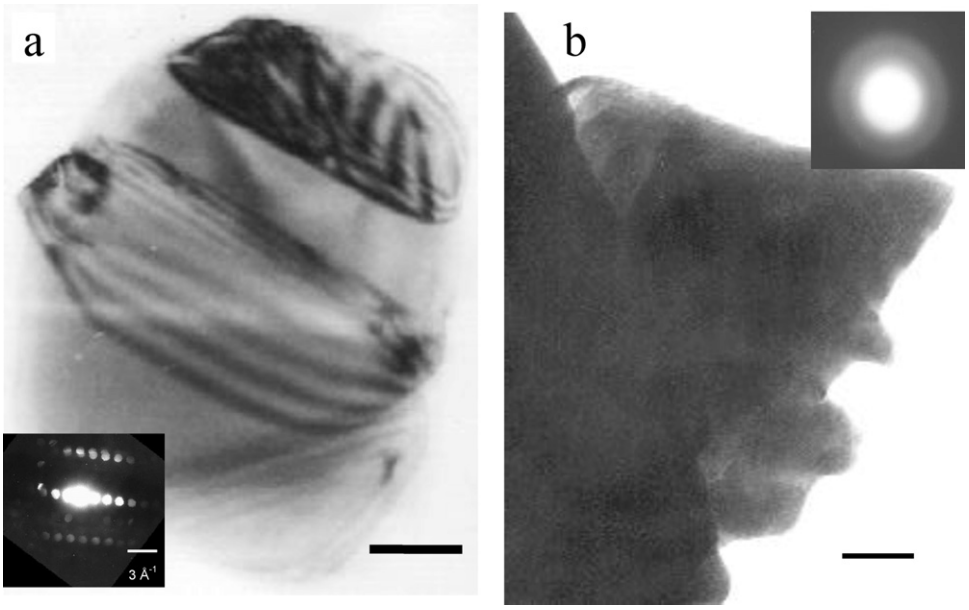

Fig. 7. TEM bright field images of (a) a C_{60} aggregate in the as milled powders of the Al/fullerene composite and (b) amorphous carbon found in the as sintered Al/graphite system. Scale bar 250 nm.

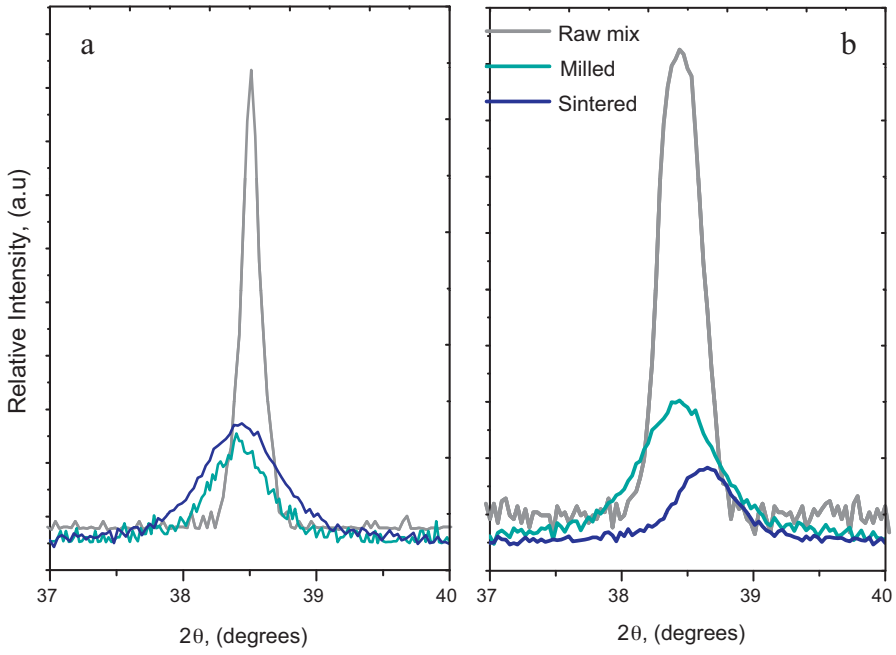

Fig. 8. XRD patterns of the original powder mixture and the as-milled (100 h) samples for (a) Al/fullerene and (b) Al/graphite systems. Note; two diffractograms for the original sample are presented to compare the advantage of using a logarithmic scale (lower) instead of a decimal scale (upper).

Al_4C_3. The fullerene mix is a cost effective manner to reinforce composites having comparable effects as those produced with pristine quality C_{60}–C_{70} or other methods involving casting or semi-solid processing [14,15]. The fullerene mix costs between 10 and 14 times less than highly pure C_{60} or C_{70} and up to 19 times cheaper than MWCNT[1].

The characterization results of XRD, SEM and TEM all show that the Al/fullerene composite has a higher volume fraction of Al_4C_3 when compared to that present in the Al/graphite composite. This is somewhat unexpected since the amount of atomic carbon is the same in both cases. However C atoms are added in different types of structures affecting the chemical activity. This most likely gives rise to the differences in the amount of carbides present in the respective composites. The determination of the reactivity of C_{60}, C_{70}, soot and graphite with Al is beyond the scope of this work; nonetheless, the current results suggest that the activity of carbon during SPS is higher for the Al/fullerene composite. Previous investigations in the literature have documented that highly pure C_{60} and C_{70}, fullerenes and CNTs have the tendency to react with Al forming Al_4C_3 [1,17–24]. Different authors, including the present ones, agree that Al has a remarkable affinity for C_{60}, C_{70},

[1] As posted on-line on 10/08/08, http://www.sigmaaldrich.com/Brands/Aldrich.html.

and fullerene-like (e.g. CNTs) structures to form carbides. However, some controversy can be raised by the findings of Kuzumaki et al. [28] that have reported a successful production of Al/CNTs composites using higher sintering and annealing temperatures than in the present work.

A quantitative analysis of the XRD results (Fig. 8) show that before and after the SPS sintering, the amount of Al_4C_3 formed in the Al/graphite or Al/fullerene composites is different. For this analysis the peaks presented in Fig. 8 have been selected and correspond to the $(1\,1\,1)_{Al}$ reflection. After mechanical alloying Fig. 8 shows a significant reduction in the intensity of the Al peaks in both systems; such a reduction is attributed to a grain refining effect during the process. However the behavior for the SPS treated powders is different for each composite. Based on the XRD intensities the $(1\,1\,1)_{Al}$ reflection increases in 7.4% in the Al/Graphite composite and decreases in 39.5% in the Al/Fullerene composite (Fig. 8b). The 7.4% increase is unexpected, since the amount of Al has not changed; therefore, this is attributed to a recrystaliztion and coarsening effects during SPS.

The intensity of the $(1\,1\,1)_{Al}$ plane in the Al/Fullerene composite shows a 39.5% reduction that is the result of the reaction among carbon an and Al along with the reduction in density (from 2.7 to 2.36 g/cm^3) for Al and Al_4C_3 respectively. If the initial amount of carbon added to the composite is taken as 15.7 at.%, based on stoichiometry the atomic percentage forming Al_4C_3 is 36.3% that corresponds to a volume of 41.9%. Based on the accuracy of the XRD apparatus this is considered precise enough to suggest that most or all carbon present in the Al/Fullerene composite transforms into Al_3C_4. If any carbon is left in the composite without transforming, the corresponding amount is untraceable by XRD means.

5. Conclusions

The fullerene mix ($C_{60} + C_{70}$ + soot) is more effective to manufacture nanostructured Al/Al_4C_3 composites than graphite. Carbon in the fullerene mix is more reactive with Al that that present in graphite. The carbon in the Al/fullerene composite transforms completely into Al_4C_3, while only partial transformation is observed for carbon in the Al/graphite composite. The milling and sintering conditions allowed to preserve the nanostructured nature of the composites. Graphite amorphization is further endorsed during mechanical alloying in the presence of Al that prevent, which somehow hinders its full transformation into carbide. The higher hardness in the Al/fullerene composite is attributed to the larger presence of Al_4C_3 in the composite. The Al matrix composites show hardness improvements of 375% and 582% for the Al/graphite and Al/fullerene composites respectively.

Acknowledgements

The authors would like to thank Drs. M. Umemoto and V. Garibay Febles for their outstanding support with mechanical alloying and Spark Plasma Sintering methods. CONACYT and SIP-COFAA-IPN are acknowledged for financial support through grants 129207 (both authors) and SIP-20110293. FCRH would like to express his gratitude to the University of Houston and the government of Texas for the start up package funding (HEAF 37215-B5008) and Dr. B. McIntyre from University of Houston for his support and discussions on this research paper.

References

[1] P.J.F. Harris, Carbon Nanotubes and Related Structures, Cambridge University Press, Cambridge, 1999.
[2] H.W. Kroto, J.R. Heath, S.C. OïBrien, R.F. Curl, R.E. Smalley, C_{60}: Buckminsterfullerene, Nature 318 (1985) 162–163.
[3] S. Iijima, Helical microtubules of graphitic carbon, Nature 354 (1991) 56–58.
[4] Q. Ru, M. Okamoto, Y. Kondo, K. Takayanagi, Attraction and orientation phenomena of bucky onions formed in a transmission electron microscope, Chem. Phys. Lett. 259 (1996) 425–431.
[5] D. Ugarte, Curling and closure of graphitic networks under electron-beam irradiation, Nature 359 (1992) 707–709.
[6] H. Terrones, M. Terrones, The transformation of polyhedral particles into graphitic onions, J. Phys. Chem. Solids 58 (1997) 1789–1796.
[7] W. Krätschmer, L.D. Lamb, K. Fostiropoulos, D.R. Huffman, C_{60}: a new form of carbon, Nature 347 (1990) 354–358.
[8] M.M. Treacy, T.W. Ebbesen, J.M. Gibson, Exceptionally high Young's modulus observed for individual carbon nanotubes, Nature 381 (1996) 678.
[9] O. Lourie, D.M. Cox, H.D. Wagner, Buckling and collapse of embedded carbon nanotubes, Phys. Rev. Lett. 81 (1998) 1638–1641.
[10] M. Umemoto, K. Masuyama, K. Raviprasad, Mechanical alloying of fullerene with metal, Mater. Sci. Forum 47 (1997) 235–238.
[11] I.I. Santana-Garcia, F.C. Robles Hernandez, V. Garibay, H.A. Calderon, Fullerene-metal composites: phase transformations during milling and sintering, solid state phenomena 172–174 (2011) 7–732.
[12] L. Sun, F. Banhart, A.V. Krasheninnikov, J.A. Rodrguez-Manzo, M. Terrones, P.M. Ajayan, Carbon, Nanotubes as high-pressure cylinders and nanoextruders, Science 312 (2006) 1199–1202.
[13] V. Garibay-Febles, H.A. Calderon, F.C. Robles-Hernández, M. Umemoto, K. Masuyama, J.C. Cabañas-Moreno, Production and characterization of (Al, Fe)-C (graphite or fullerene) composites prepared by mechanical alloying, Mater Manuf. Process. 15 (2000) 547–567.
[14] F. Adams, C. Vivès, Die-casting under low pressure of electromagnetically elaborated semisolid metal matrix composites, Netherlands Soc. Mater. Sci. 1 (1997) 337.
[15] F.C. Robles Hernández, J.H. Sokolowski, Comparison among chemical and electromagnetic stirring and vibration melt treatments for Al–Si hypereutectic alloys, J. Alloys Compd. 426 (2006) 205.
[16] D.M. Hulbert, D. Jiang, U. Anselmi-Tamburini, C. Unuvar, A.K. Mukherjee, Experiments and modeling of spark plasma sintered, functionally graded boron carbide–aluminum composites, Mater. Sci. Eng. A 488 (2008) 333–338.
[17] J.S. Benjamin, in: E. Arzt, L. Schultz (Eds.), New materials by mechanical alloying techniques, DGM Informationgesellschaft, Oberursel, Germany, 1989, p. 3.
[18] P.S. Gilman, J.S. Benjamin, Mechanical Alloying, Annu. Rev. Mater. Sci. 13 (1983) 279.
[19] C. Suryanarayana, Prog. Mater. Sci. 46 (2001) 1–184.
[20] J. Guerrero-Paz, F.C. Robles-Hernández, R. Martínez-Sánchez, D. Hernández-Silva, D. Jaramillo-Vigueras, Particle size evolution in non-adhered ductile powders during the mechanical alloying, Mater. Sci. Forum 360–362 (2001) 317–322.
[21] M. Umemoto, Z.G. Liu, K. Masuyama, K. Tsuchiya, Ball mill of fullerene and mechanical alloying of fullerene-metal systems, Mater. Sci. Forum 312–314 (1999) 93–102.
[22] F.C. Robles Hernández, H.A. Calderón, "Synthesis of fullerene on Fe-C composites by Spark Plasma Sintering and its thermomechanical transformation to diamond", MRS Proceedings 1243 (2010) 5.
[23] Z.G. Liua, H. Ohi, K. Masuyama, K. Tsuchiya, M. Umemoto, Mechanically driven phase transition of fullerene, J. Phys. Chem. Solids 60 (2000) 1119–1122.
[24] M. Umemoto, K. Masuyama, K. Tsuchiya, Mechanical alloying of fullerene with various metal elements, Mater. Sci. Forum 269 (1998) 31–36.
[25] R. Pérez-Bustamante, C.D. Gómez-Esparza, I. Estrada-Guel, M. Miki-Yoshida, L. Licea-Jiménez, S.A. Pérez-García, R. Martinez-Sanchez, Microstructural and mechanical characterization of Al-MWCNT composites produced by mechanical milling, Mater. Sci. Eng. A 502 (2009) 159–163.
[26] M. Oda, C. Masuda, F. Ogawa, S. Itabashi, T. Nishimura, TMS. Annual Meeting and Exhibition, San Francisco, Conference Proceedings, TMS International, 2009.
[27] E.J. Lavernia, Z. Zhang, F. Zhou, On the analysis of grain size in bulk nanocrystalline materials via X-ray diffraction, Metall. Mater. Trans. A: Phys. Metall. Mater. Sci. 34A: (2003) 1349–1355.
[28] T. Kuzumaki, K. Miyasawa, H. Ichinose, K. Ito, Processing of carbon nanotube reinforced aluminum composite, J. Mater. Res. 13 (1998) 2445–2449.
[29] L. Ci, Z. Ryu, N.Y. Jin-Phillipp, M. Rhüle, Investigation of the interfacial reaction between multi-walled carbon nanotubes and aluminum, Acta Mater. 54 (2006) 5367–5375.
[36] Y. Hu, O.A. Shenderova, Z. Hu, C.W. Padgett, D.W. Brenner, Carbon nanostructures for advanced composites, Rep. Prog. Phys. 69 (2006) 1847–1896.
[40] F.C. Robles Hernández, H.A. Calderon, Nanostructured metal composites reinforced with fullerene, JOM 62 (2) (2010) 63–68.